

Delayed Post-Injury Administration of Riluzole Is Neuroprotective in a Preclinical Rodent Model of Cervical Spinal Cord Injury

Yongchao Wu,^{1,*} Kajana Satkunendrarajah,^{1,*} Yang Teng,² Diana S.-L. Chow,²
Josef Buttigieg,^{1,**} and Michael G. Fehlings^{1,3}

Abstract

Riluzole, a sodium/glutamate antagonist has shown promise as a neuroprotective agent. It is licensed for amyotrophic lateral sclerosis and is in clinical trial development for spinal cord injury (SCI). This study investigated the therapeutic time-window and pharmacokinetics of riluzole in a rodent model of cervical SCI. Rats were treated with riluzole (8 mg/kg) at 1 hour (P1) and 3 hours (P3) after injury or with vehicle. Afterward, P1 and P3 groups received riluzole (6 mg/kg) every 12 hours for 7 days. Both P1 and P3 animals had significant improvements in locomotor recovery as measured by open field locomotion (BBB score, BBB subscore). Von Frey stimuli did not reveal an increase in at level or below level mechanical allodynia. Sensory-evoked potential recordings and quantification of axonal cytoskeleton demonstrated a riluzole-mediated improvement in axonal integrity and function. Histopathological and retrograde tracing studies demonstrated that delayed administration leads to tissue preservation and reduces apoptosis and inflammation. High performance liquid chromatography (HPLC) was undertaken to examine the pharmacokinetics of riluzole. Riluzole penetrates the spinal cord in 15 min, and SCI slowed elimination of riluzole from the spinal cord, resulting in a longer half-life and higher drug concentration in spinal cord and plasma. Initiation of riluzole treatment 1 and 3 hours post-SCI led to functional, histological, and molecular benefits. While extrapolation of post-injury time windows from rat to man is challenging, evidence from SCI-related biomarker studies would suggest that the post-injury time window is likely to be at least 12 hours in man.

Introduction

ACUTE SPINAL CORD INJURY (SCI) is a catastrophic neurological trauma. The incidence of SCI has been estimated to range between 15 and 40 individuals per million globally.¹ SCI initially results in mechanical damage to neurons and supporting cells, followed by expansion of the initial injury via a cascade of events that lasts days to months.^{2,3} At present, there is still a lack of effective therapeutic strategies for the treatment of SCI. Many therapeutic strategies have shown functional and histological improvements in animal models of SCI with only limited success in human clinical trials.⁴

Riluzole, a neuroprotective drug licensed for the treatment of amyotrophic lateral sclerosis (ALS) patients, has also been tested in a rat model of SCI in a number of laboratories, including our own.^{5,6} Riluzole acts on multiple molecular targets to improve

functional recovery, although its mechanism of action has not been fully delineated.^{6,7} Riluzole may offer neuroprotection after SCI by reducing excitotoxicity via the inhibition of presynaptic glutamate release.⁹ Following experimental SCI, riluzole has been shown to be neuroprotective, leading to preserved axonal integrity through the lesion epicenter, reduced cavitation, decreased calpain activation, subsequent reduction in proteolysis of cytoskeletal substrates,¹⁰ and improved neurobehavioral outcomes.^{11,12} Mu and associates also reported that riluzole, in combination with methylprednisolone sodium succinate (MPSS), resulted in significant increases in spared tissue and locomotor function.¹³ Based on these promising experimental results in animal models of SCI and an excellent safety profile in ALS, riluzole is currently in a Phase I clinical trial for the treatment of SCI.

The clinical trial has been established to assess the effects of riluzole in patients with SCI between neurological levels C4 and

¹Toronto Western Research Institute and Krembil Neuroscience Centre, and ³Division of Neurosurgery, University Health Network, University of Toronto, Toronto, Ontario, Canada.

²College of Pharmacy, University of Houston, Houston, Texas.

*Joint first authors.

**Affiliation at time of work. Current affiliations: Yongchao Wu, Huazhong University of Science and Technology, China; Josef Buttigieg, University of Regina, Saskatchewan, Canada.

T12. Patients will receive the first dose of 50 mg within 12 hours of injury, then further doses twice daily for 14 days, with the same doses used in ALS patients. A 14-day course was chosen, since glutamate and sodium-mediated secondary injury is maximal during this period.^{3,5}

However, despite the fact that riluzole is already at the stage of clinical trials, there are key challenges remaining before it can be fully and safely translated into the clinic. First, the effective time window within which riluzole can be administered post-SCI has not been investigated preclinically. Riluzole has been shown to be effective when administered 15 minutes after SCI in rodents.¹² A time window of 2 hours has been studied in combination with MPSS. However, as MPSS is only standard protocol for SCI in some hospitals, it is essential to determine the optimal time window for riluzole treatment on its own.

A second concern relates to the fact that more than 60% of all spinal cord injuries occur at the cervical level.¹⁴ Cervical SCI results in higher mortality, mainly due to cardio-pulmonary complications.¹⁵ Hence, there is tremendous value in testing riluzole in an animal model of cervical SCI. The pharmacokinetic profile of riluzole following SCI has never been investigated. Circulatory status is altered following SCI;¹⁵ therefore, it is not possible to simply extrapolate the pharmacokinetic data from healthy or ALS subjects to those with SCI.

Resolving the key challenges mentioned above will facilitate the translation of riluzole for the treatment of SCI. The current study aims to address these challenges by determining the therapeutic time window for riluzole administration post-SCI and by determining the pharmacokinetic profile of riluzole in a rodent model of cervical SCI.

Methods

Spinal cord injury model

All experimental protocols were approved by the animal care committee at the University Health Network (Toronto). Female Wistar rats (250–300 g; Charles River, Canada) under isoflurane anesthesia (2%) were subjected to C7–T1 laminectomy. The spinal cord at C7–T1 was compressed extradurally for 1 min between 1 mm blades of a modified aneurysm clip calibrated to deliver a closing force of 35 grams. This injury resulted in moderate SCI, as described previously.¹⁶ All animals received analgesic (buprenorphine 0.05 mg/kg) postsurgically and 5 mL of saline. Animals were housed in individual cages and given food and water ad libitum. The rats were maintained in a 12-hour light/dark cycle at a temperature of 26°C. Manual expression of their bladders was performed three times daily until a reflex bladder was established.

Drug preparation and administration

Drug concentrations and administration profiles were selected based on previously reported pharmacodynamic and kinetic properties of systemically administered riluzole reported.^{11,13} Riluzole (Sigma, R116) was dissolved in 30% (w/v) of solubilizer 2-hydroxypropyl- β -cyclodextrin (HBC, Sigma, H-107), resulting in a final concentration of 8 mg/mL, followed by 0.22 μ m syringe filtration.

In order to determine the ability of cervical spinal cord-injured rats to tolerate repeated administration of riluzole, 8 mg/kg ($n=6$), 6 mg/kg ($n=10$), or 4 mg/kg ($n=6$) of riluzole was administered intraperitoneally (IP) 1 h after injury and every 12 h for 7 days. The animals were closely monitored daily, for any changes in overall health and the mortality rate was calculated. A group of uninjured rats also received riluzole (8 mg/kg; IP) every 12 h for 7 days.

Subsequently, to test the therapeutic time window of riluzole, a set of injured rats was randomly assigned to one of the following three groups ($n=12$ /group): injected IP with 8 mg/kg of riluzole at 1 h (P1 group) or 3 h (P3 group) post-injury, or received HBC medium (control group). After the initial dose, animals in the P1 and P3 groups received 6 mg/kg of riluzole IP every 12 h for 7 days, while rats in the control group were given HBC.

Behavioral testing

Neurobehavioral recovery after SCI in P1, P3, and control animals was assessed from weeks 1 to 6 post-injury. Locomotor recovery of the animals was assessed weekly by two independent blinded observers using the 21-point BBB open field locomotor score.¹⁷ The BBB scale was used to evaluate hindlimb locomotor recovery, including joint movements, stepping ability, coordination, and trunk stability. Scores were averaged across both the right and left hindlimbs.

In addition, BBB subscore tests were performed at the sixth week after injury to improve the sensitivity of the BBB score by scoring some of the behavioral attributes independently. The BBB subscore is a 7-point scale that evaluates toe clearance, paw position, stability, and tail position with 7 representing normal function.

The gridwalk analysis was used to assess sensory-motor coordination of the limbs.¹⁸ The gridwalk assessment requires accurate paw placement and substantial motor control to cross a meter long runway of round metal bars. The metal bars are spaced unevenly to avoid habituation. All animals had three training sessions on the gridwalk. For each test session, animals had to cross the runway three times. No reinforcement was given after the sessions. The sessions were videotaped and analyzed offline in slow motion. In particular, the number of footfalls within the defined 20 bar section was counted. The injured rats with dragging hindlimbs were scored the maximum footfalls of 20. Due to the loss of weight support after injury, gridwalk analyses started 3 weeks after injury when most of the injured rats were able to support their weight sufficiently.¹⁹

All rats were assessed for mechanical allodynia at 6 weeks post-SCI to evaluate neuropathic pain.^{20,21} In brief, mechanical allodynia was assessed by applying 10 stimuli using 2 g von Frey filament to the dorsal neck, trunk, around the site of lesion and paws. Each stimulus lasted 3 sec, followed by a 5 sec interval. The number of avoidance responses (trunk shakes, jumping, escaping, vocalization, or aversive reactions) was recorded.

Retrograde axonal tracing

Retrograde axonal tracing with fluorogold was performed to evaluate the integrity of descending axons. The fluorescent tracer fluorogold (FG, Chemicon) was dissolved in distilled water to a final concentration of 4% and filter sterilized through a 0.22 μ m filter. The technique for placement of the axonal tracer is similar to that described in previous reports from our laboratory.¹² Five animals from each group underwent complete spinal transection at T10. One sterile gelfoam (2×5×5 mm) saturated with the fluorogold solution was placed between the rostral and caudal ends of the transected cords to ensure maximal exposure of the rostral surfaces of the transected cords to the fluorogold solution. The transected ends and gelfoam were covered with petroleum jelly to avoid diffusion of fluorogold. One week after the fluorogold implantation, the brain and spinal cord were extracted after transcardial perfusion fixation. Serial frozen 30 μ m sections were cut in the coronal plane through the brainstem, and every third section was collected. All sections were viewed under fluorescence microscope to quantify the number of retrogradely labeled neurons. Fluorogold-labeled neurons in the reticular nuclei, vestibular nuclei, and red nucleus were identified according to the rat brain atlas (George Paxinos, Charles Watson). All labeled neurons in these areas were counted.

Immunohistochemistry

Animals were perfused transcardially with 4% paraformaldehyde in PBS at 6 weeks after SCI. The tissues were cryoprotected in 20% sucrose in PBS and the spinal cord segments (1 cm length) centered at the injury site were embedded in mounting medium, frozen, and sectioned on a cryostat at a thickness of 20 μm . Serial spinal cord sections were stained with the myelin-selective stain luxol fast blue (LFB) and the cellular stain hematoxylin–eosin (HE) to identify the injury epicenter. Tissue sections displaying the largest proportion of cavity and scar in whole cross-sectional area were taken as being the focal point of the injury epicenter.

Tissue sparing was analyzed from 1200 μm rostral to 1200 μm caudal to the epicenter, at intervals of 400 μm . Tissue sampling was done at equivalent distance from the epicenter for each spinal cord. The LFB/HE stained sections were taken using a Leica fluorescence microscope with Stereo Investigator. The measurements were carried out using ImageJ software (National Institutes of Health). Cross-sectional residual tissue was normalized to the entire cross-sectional area. Normal gray and white matter areas devoid of any pathology such as cavitation, fibrosis, and necrosis were included.

The following primary antibodies were used: anti-NeuN (1:500; Chemicon, for neurons, anti-GFAP (1:500; Chemicon) for astrocytes, mouse anti-APC (CC1, 1:100; Calbiochem) for oligodendrocytes, anti-NF 200 (1:200; Sigma) for axons; anti-chondroitin sulfate antibody (CS-56, 1:100, Sigma) for chondroitin sulfate proteoglycan (CSPG); Iba-1 (1:500, Wako) for macrophages/microglia.²²

The sections were rinsed three times in PBS after primary antibody incubation overnight at 4°C for 2 h at room temperature, and then incubated with fluorescent secondary antibody Alexa 568, 647, or 488 (1:400; Invitrogen) for 1 h. The sections were again rinsed three times with PBS and coverslipped with Mowiol mounting medium containing DAPI (Vector Laboratories) to counterstain the nuclei. The images were taken using a Zeiss 510 laser confocal microscope and Leica fluorescence microscope with Stereo Investigator.

For assessment of inflammation and scar formation in the spinal cords, the sections were stained with Iba1 (a marker of activated microglia and macrophages), GFAP and CSPG antibodies. Images of the whole cross-sections were taken with Leica fluorescence microscope with Stereo Investigator. The measurements of the integrated density were carried out using ImageJ.

TUNEL staining

To determine the ability of riluzole treatment to prevent apoptotic cell death after SCI, terminal deoxynucleotidyl transferase-mediated dUTP nick end labeling (TUNEL) staining was performed with an ApoTag kit (Chemicon) on sections 700 μm caudal from the epicenter of samples collected 7 days after injury ($n=5$).²³ Briefly, sections were processed in a solution of 2:1 ethanol-acetic acid (Fisher Scientific) at -20°C for 5 min. Afterward, sections were rinsed three times in PBS, once in equilibration buffer, followed by application of terminal deoxynucleotidyl transferase enzyme for 1 h in a humidified chamber at 37°C. To label apoptotic cells, an anti-digoxigenin-fluorescein conjugate solution was applied to sections for 1 h at room temperature in the dark. Slides were mounted and coverslipped with Mowiol containing DAPI. As a negative control for TUNEL, reaction buffer alone (terminal deoxynucleotidyl transferase enzyme omitted) was used, followed by fluorescent secondary antibody. Each section was imaged using a Leica microscope with Stereo Investigator and the number of TUNEL positive cells was counted.

Western blot analysis

Preservation of the axonal cytoskeleton was assessed by Western blot analysis. A 5-mm length of the spinal cord centered at the injury epicenter was quickly dissected on a chilled stage and

immediately transferred to a microcentrifuge tube containing 200 μL of protein homogenization, ground, and centrifuged for 15 min at 20,000 g at 4°C. Protein concentration was determined using the Lowry protein assay. Protein samples consisting of 20 μg were loaded into 7.5% polyacrylamide gels (Bio-Rad) and electroblotted onto nitrocellulose membranes. Membranes were probed with monoclonal anti-NF200 antibody (1:2000; Sigma, N0142) for 1 h at room temperature. The membranes were then incubated with a 1:2000 dilution of goat anti-mouse horseradish peroxidase conjugated secondary antibodies (1:10,000, Sigma). The bands were blotted with an enhanced chemiluminescence (ECL) detection system (Perkin Elmer). Beta-actin (Chemicon) was immunoblotted as a loading control. Gel-Pro Plus Analyzer software (Media Cybernetics) was used for integrated optical density (OD) analysis.

Electrophysiology

Sensory evoked potentials (SEPs) were recorded from 18 rats that had undergone SCI, as well as 6 uninjured rats under isoflurane anesthesia. The rats were immobilized in the prone position and fixed in a stereotaxic holder. The intervertebral ligaments between C1 and C2 were removed surgically using fine forceps. Two pairs of 1.0 mm ball electrodes were positioned extradurally over the spinal cord at C1 and C2 for recording evoked potentials. The sciatic nerve was exposed, desheathed, and placed on bipolar silver electrodes. A constant current stimulus of 0.1 ms in duration and 2.0 mA in intensity was applied at a rate of 5.7 Hz to the sciatic nerve. At a bandwidth of 10 to 3000 Hz, a total of 2000 SEPs were averaged and replicated. SEPs peak latency was measured from the start of the stimulus to the peak of first negative peak (N1). The evoked potential amplitudes were measured as the voltage difference from the peak of first positive peak to the peak of the negative peak (N1).

Pharmacokinetics

A total of 50 rats were used for this experiment. Two groups of rats underwent cervical SCI, while two other groups were age-matched uninjured rats. In SCI rats, two different riluzole treatment protocols were used post SCI. The first SCI group received a single dose of riluzole at 8 mg/kg (IP) and had blood and cervical and thoracic segments of the spinal cord extracted at 15 min, 30 min, 1 h, 3 h, or 9 h ($n=4$ for each time point). Blood and spinal segments from an uninjured group were also collected at the same time points. Two other groups, one group of injured and one of uninjured rats, received multiple doses of riluzole with an initial dose of 8 mg/kg followed by 6 mg/kg riluzole every 12 h for 3 days ($n=5$ /group). Blood samples and spinal cord segments from the cervical and thoracic regions were collected 2 h after the last injection (the sixth dose) from both groups. The plasma samples of 500 μL were collected by adding 100 μL of 50 mM EDTA to 1 mL of whole blood and centrifuging at 3000 g for 10 min at 4°C.

Riluzole was extracted from plasma, brain, and spinal cord samples with ethyl acetate. Riluzole was assayed using a validated high performance liquid chromatography (HPLC) method with UV detection at 263 nm.²⁴ Baseline resolution was achieved on Waters Symmetry® C18 column (3.0 \times 150 mm, 3.5 μm) with Symmetry® C18 guard column (2.1 \times 10 mm, 3.5 μm), eluted at the flow rate of 0.45 mL/min, with the mobile phase of acetonitrile:methanol:0.1 M ammonium acetate (3:2:5, v/v/v), adjusted with acetic acid to pH 6.5. The retention times of riluzole and internal standard (5-methoxyorsoralen, 5-MOP) were 6.9 and 8.9 min, respectively. The HPLC assay was validated with less than 10% of intraday and interday variability and a linearity of 7.8–1,000 ng/mL for the plasma samples and 31.25–4,000 ng/g for the brain and spinal cord samples. The lower limits of quantification were 7.8 ng/mL for plasma and 31.25 ng/g for brain and spinal cord.

Statistical analysis

Data were analyzed with SigmaStat software (Systat Software Inc) and Graphpad Prism (GraphPad Software). For comparison of groups over time (BBB behavioral testing) or distance (tissue sparing), two-way analysis of variance (ANOVA) with repeated measures was used, followed by the post-hoc Bonferroni test. For comparison of simple effects, one-way ANOVA followed by the post-hoc Bonferroni test was applied. In all results and figures, the mean \pm SEM are used to describe the results. Statistical significance was set at $p < 0.05$.

Results

Tolerance of rats with cervical SCI to repeated administration of riluzole

A one-time administration of 8 mg/kg (IP) of riluzole has been shown to be neuroprotective following SCI in our lab.⁵ However, repeated administration of 8 mg/kg of riluzole was not well tolerated in rats with cervical SCI in the present study. Seven out of the 10 animals treated with this dose died within 1 week of drug administration, and the majority of these animals died between 2 and 4 days after SCI. All rats appeared lethargic for the entire duration of riluzole treatment. All rats on repeated doses of 8 mg/kg experienced respiratory distress prior to death. However, the administration of the same dose of riluzole in uninjured rats did not result in any observable adverse effects. The injured group of rats that received 6 mg/kg of riluzole had an overall survival rate of 92.3% (24/26). Furthermore, all rats in the above group did not display any

respiratory distress. 4 mg/kg of riluzole was well tolerated by all animals treated at this dose level and significant lethargy due to the treatment was not observed. This initial experiment revealed that 6 mg/kg of riluzole is tolerated well without significant mortality. Based on the above results, 6 mg/kg of riluzole was used to determine the therapeutic time window of riluzole for the treatment of SCI.

Riluzole promotes neurobehavioral recovery after SCI

All animals were incompletely paraplegic immediately post-SCI with progressive recovery of some hindlimb function over 6 weeks. Immediately after injury, most animals were only able to display extensive joint movements. Animals in all groups had gradual improvements in locomotor function that plateaued after 4 weeks in all injured rats, indicating a progression in recovery from an early to intermediate phase. Two-way ANOVA revealed significant improvements in BBB score in both P1 and P3 groups of rats compared to control. From the second to the sixth week post-injury, riluzole treatment an hour post-injury (P1) showed a statistically significant improvement in BBB scores compared to the control group (Fig. 1A). At 6 weeks, the control rats reached an average score of 10.25 ± 0.41 . In contrast, the P1 rats reached an average score of 11.42 ± 0.15 , showing significant functional improvement ($p = 0.011$). The rats treated with riluzole 3 h post-SCI (P3) showed an overall improvement in BBB score compared to control ($p = 0.021$), although post hoc testing did not show significant differences from control at 4, 5, and 6 weeks post-injury.

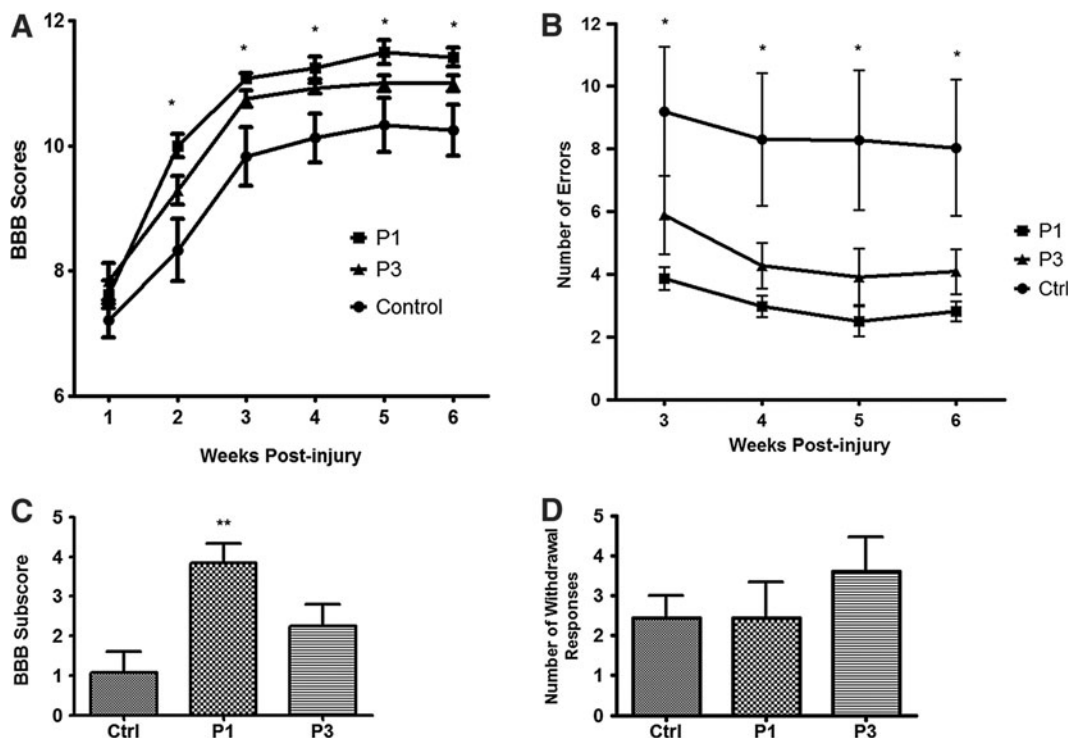


FIG. 1. Riluzole promotes locomotor recovery after SCI in rats. (A) Riluzole treatment 1 h post-injury (P1) provided the greatest improvements in BBB scores compared to vehicle-treated control group from second to sixth week post-injury ($p = 0.003$). The group treated with riluzole 3 h post-SCI (P3) showed significant behavioral improvements compared to control group ($p = 0.014$). (B) BBB subscore confirmed the neuroprotective effect of riluzole (P1) compared to vehicle-treated control ($p = 0.003$). P3 group did not show significant improvements ($p = 0.141$). (C) Gridwalk analysis revealed sensory-motor recovery in the P1 group from weeks 3 to 6 after injury with reduced number of footfalls ($p = 0.026$), while the P3 group had a trend toward a decrease in the number of footfalls that did not reach significance ($p = 0.098$). (D) Mechanical allodynia did not increase in response to treatment. Data are expressed as mean \pm SEM. * $p < 0.05$, ** $p < 0.01$.

BBB subscores confirmed the neuroprotective effects of riluzole treatment initiated at 1 h post-injury. The P1 group had a significantly higher subscore of 3.83 ± 0.51 , while the vehicle-treated controls scored 1.08 ± 0.53 ($p=0.003$) (Fig. 1C). The group that had riluzole treatment initiated at 3 h post-SCI had a BBB subscore of 2.25 ± 0.55 ($p=0.065$). Although the P3 group had a higher subscore compared to controls, it did not reach significance. This experiment demonstrated that P1 (i.e., early administration post-injury) is the optimal time for initiating riluzole treatment post-SCI in this animal model.

Grid walk analysis revealed an overall improvement in sensory and motor function from weeks 3 to 6 post-injury in both P1 and P3 groups of rats (Fig. 1B). At 6 weeks after SCI, the average number of footfalls in the P1 group was 2.81 ± 0.32 compared to 8.04 ± 2.17

footfalls in the control group ($p=0.026$). The P3 group showed a trend of reduced footfalls of 4.08 ± 0.72 , which failed to reach significance ($p=0.065$).

At 6 weeks post-injury, the response to Von Frey stimuli (at level and below the injury level) remained unchanged in both riluzole-treated groups and the vehicle-treated animals. Mechanical allodynia did not increase as the sensory-motor function improved (Fig. 1D).

Electrophysiology

Changes in axonal function were examined using SEPs. SEP amplitude was significantly greater in both riluzole treated groups (P1, P3) compared to vehicle-treated control groups. Peak

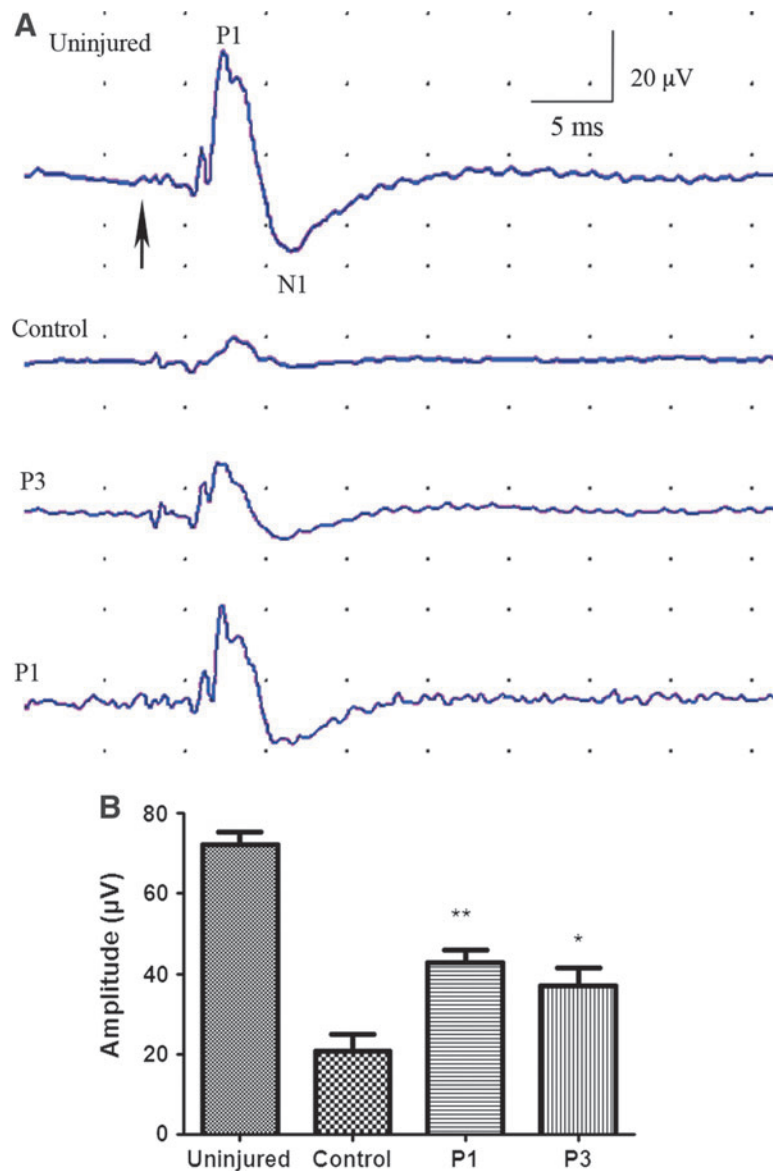


FIG. 2. Sensory evoked potentials (SEPs). SEPs peak latency was measured from the start of the stimulus (A, arrow) to the first negative peak (N1). The evoked potential amplitudes were measured as the voltage difference from the peak of first positive peak (P1) to the peak of the negative peak (N1). Peak amplitude of SCI rats that received riluzole 1 and 3 h post-injury were $42.67 \pm 3.355 \mu\text{V}$ ($p=0.004$) and $37.00 \pm 4.555 \mu\text{V}$, ($p=0.046$), respectively. Riluzole-treated rats had significantly higher peak amplitude than control ($20.67 \pm 4.25 \mu\text{V}$). The SEP latencies were not significantly different among groups.

amplitude was $42.67 \pm 3.36 \mu\text{V}$ ($p=0.004$) and $37.00 \pm 4.56 \mu\text{V}$ ($p=0.046$) in the P1 and P3 groups, respectively, while those treated with HBC had peak amplitudes of $20.67 \pm 4.25 \mu\text{V}$ (Fig. 2). Peak latencies were not significantly different among groups.

Riluzole enhances tissue preservation following cervical SCI

Six weeks after SCI, spinal cord cross-sections were stained serially with LFB/HE. Spinal cords from rats treated with riluzole 1 h post-injury exhibited a greater degree of spared tissue at the injury epicenter compared to tissue sections from control rats (Fig.

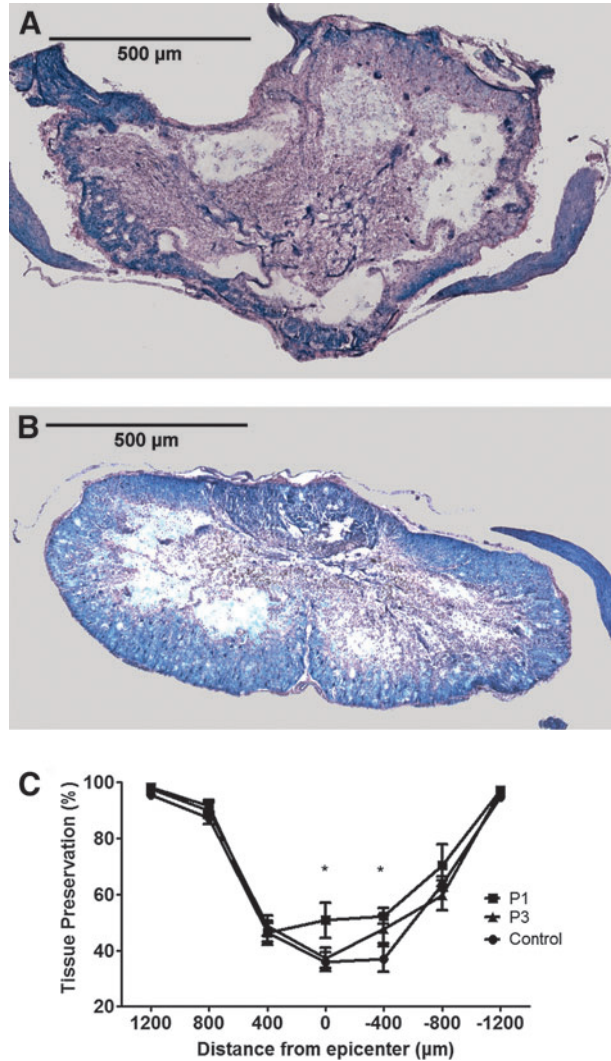


FIG. 3. Riluzole enhances tissue preservation following cervical SCI. Spinal cord cross-sections were stained serially with LFB/HE. Representative images taken from the injury epicenter of control (A) and P1 (B). Measurements of residual tissue taken from cross-sectional areas were expressed as a percent of the total cross-section area of the section (C). This experiment revealed a significant improvement in tissue preservation in the riluzole-treated groups. The percentage of remaining tissue was $50.74 \pm 6.41\%$ in P1 and $35.99 \pm 3.30\%$ in control at injury epicenter ($p=0.014$). At $400 \mu\text{m}$ caudal to the injury epicenter, the P1 group had significantly more preserved neural tissue ($52.28 \pm 2.74\%$) compared to control ($36.98 \pm 4.56\%$) ($p=0.010$).

3A and B, respectively). A comparison of percent normalized residual tissue was performed by two-way ANOVA assessing treatment and distance from the injury epicenter (Fig. 3C). Overall, there was a significant improvement in tissue preservation in the P1 group ($p=0.014$). At 6 weeks post-injury, percentage of remaining tissue was $50.74 \pm 6.41\%$ in P1 group and $35.99 \pm 3.30\%$ in vehicle-treated controls at the injury epicenter ($p=0.014$). Similarly, there was a significant increase in preserved neural tissue at $400 \mu\text{m}$ caudal to the epicenter in the P1 group ($52.28 \pm 2.74\%$) compared to vehicle-treated controls ($36.98 \pm 4.56\%$) ($p=0.010$).

Riluzole treatment enhanced axonal integrity across the lesion epicenter

Retrogradely labeled FG-positive neurons in key brainstem nuclei were counted to assess the survival of descending axons traversing the lesion (Fig. 4). The medullary reticular nuclei (ventral and dorsal reticular fields and caudal and rostral pontine reticular nuclei), vestibular nuclei (median, lateral, superior, and inferior vestibular nuclei), and the red nuclei (magnocellular and parvocellular) were assessed for FG-positive neurons. FG-positive neurons in the medullary reticular formation in both the P1 and P3 groups were significantly higher compared to control. The groups that received riluzole at 1 and 3 hour post-SCI had 2052.4 ± 65.14 and 2362.2 ± 221.32 medullary reticular neurons, respectively, whereas the injured control group only had 1494.2 ± 83.6 neurons. The vestibular nuclei (median, lateral, superior, and inferior vestibular nuclei) and the red nuclei (magnocellular and parvocellular) were assessed for FG-positive neurons. Representative fluorescent photomicrographs of retrograde FG-labeled neurons within medullary reticular nuclei derived from P1 and control rats are shown in Figure 4A and B, respectively. A significant increase of FG-positive somas in the vestibular nuclei was observed in P1 rats ($p=0.009$) (Fig. 4C) but not in P3. The number of FG-positive somata from the vestibular nuclei of vehicle-treated and P1 and P3 groups was 424.2 ± 30.73 , 777.0 ± 70.04 and 480.2 ± 100.7 , respectively. FG-positive somas within the red nuclei ($p=0.153$) of treated animals were not significantly different from control (Fig. 4D). The red nuclei of vehicle-treated, P1, and P3 groups were 820 ± 77.50 , 1067 ± 127.8 , and 1025 ± 98.79 , respectively. The number of FG-positive neurons in the vestibular nuclei of riluzole-treated rats was not significantly higher than those in vehicle-treated controls ($p=0.056$).

Riluzole treatment preserves cytoskeletal integrity of axons

In this study, cytoskeletal integrity of the cervical (C7) spinal cord was assessed. Homogenates of 5 mm of spinal cord around the lesion epicenter were used for Western blot analysis of the cytoskeletal protein neurofilament 200 (NF200). It has been demonstrated that after SCI, calcium-mediated excitotoxicity leads to the degradation of NF200.²⁵ Spinal cord-injured rats who received riluzole treatment had less NF200 degradation compared to vehicle-treated controls (Fig. 5A). At 1 week post-injury, densitometric values of NF200 (which were normalized by the values of β -actin) for control, P1, and P3 were 0.182 ± 0.046 , 0.755 ± 0.165 , and 0.304 ± 0.084 , respectively (Fig. 5B). P1 rats exhibited a higher relative amount of NF200 as compared to controls ($p=0.005$).

Riluzole reduces inflammation in SCI

Many neuropathological changes observed after SCI are associated with the breakdown of the blood–spinal cord barrier and the

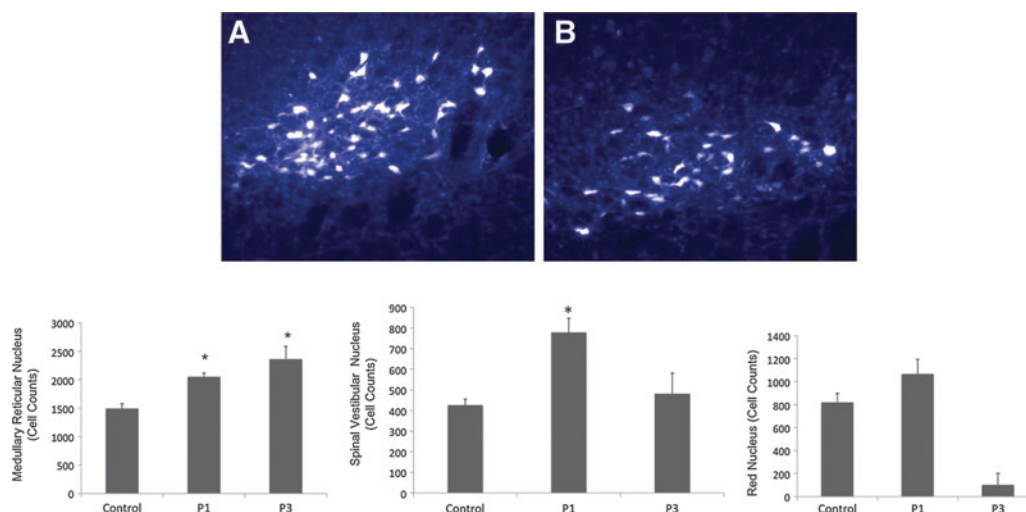


FIG. 4. Retrograde tracing of neurons with fluorogold. Representative images of fluorogold-labeled neurons within the vestibular nuclei. Fluorogold-labeled neurons from control (A) and P1 (B) animals at 7 weeks post-SCI. Quantification of preserved fluorogold-positive brainstem neurons demonstrated that riluzole treatment at 1 and 3 h post-injury is associated with an increased preservation of axons through the lesioned cord compared to control. Medullary reticular nucleus of P1 and P3 groups had significantly higher number of neurons compared to control. Vestibular nuclei of P1 group contained a significantly higher number of labeled neurons compared to control. The number of FG-positive neurons within the red nuclei of control and riluzole-treated groups were not significantly different. Data are expressed as mean \pm SEM. * denotes a significantly greater number of neurons compared to control ($p < 0.05$; $n = 6$).

infiltration of macrophages accompanied by the activation of microglia, the resident CNS immune cells. Using Iba1, which is a marker for activated microglia/macrophage, the effect of riluzole on the immune response after cervical SCI was examined. A significant decrease in Iba1-positive macrophages and microglia were observed in spinal cord samples taken 1 week post-injury from P1

compared to vehicle-treated controls (Fig. 6A and B, respectively). The integrated density of Iba1-positive cells in P1 animals was 125.00 ± 34.94 while the vehicle-treated controls was 355.80 ± 76.0 ($p = 0.033$) (Fig. 6C). P3 animals had optical density of 193.20 ± 43.00 , which was also significantly lower than those in controls ($p = 0.05$).

Similar results were observed at 6 weeks post-injury. Optical density was 312.8 ± 78.47 , 78.48 ± 9.697 , and 130.3 ± 12.40 in control, P1, and P3 groups, respectively (Fig. 6D). Both P1 and P3 groups had significantly lower Iba-1 at 6 weeks post injury (P1: $p = 0.008$; P3: $p = 0.041$).

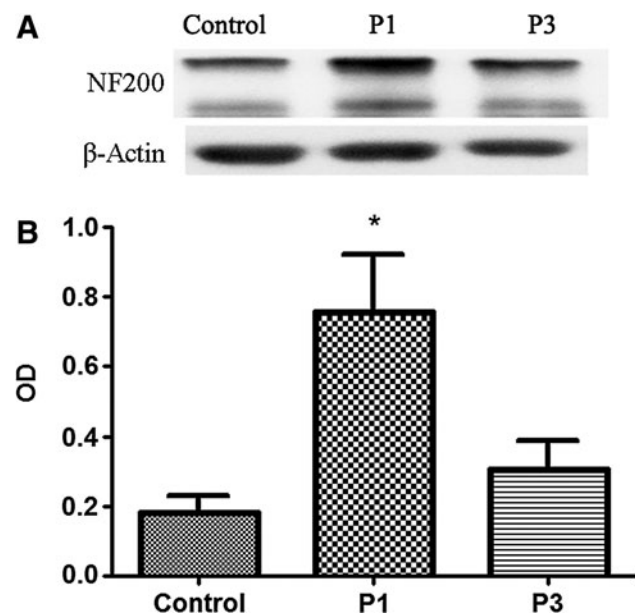


FIG. 5. Western blot analysis of neurofilament degeneration. (A) Representative Western blot demonstrating the protein expression profiles for 200 kd neurofilament (NF200) and β -actin from spinal cord-injured animals with and without riluzole treatment. (B) Histogram displaying the ability of riluzole treatment at 1 h post-SCI (P1) to reduce the loss of the NF200.

Riluzole reduces apoptosis

TUNEL-positive cells were found throughout the gray and white matter in the injured spinal cord (Fig. 7A and B). An overall apoptotic cell count value was obtained from 5 animals each in control and riluzole-treated groups. Apoptotic cells counts from control, P1, and P3 groups were 374.20 ± 82.01 , 129.80 ± 18.35 , and 260.00 ± 42.87 , respectively. As shown in Figure 7C, statistical analysis demonstrated a significant riluzole-mediated protective effect in the P1 group ($p = 0.024$); however, the reduction in apoptosis in the P3 group did not achieve significance ($p = 0.492$) compared to control (Fig. 7C). A portion of apoptotic cells in the white matter was co-localized with CC1-labeled oligodendrocytes (Fig. 7D–G).

Pharmacokinetic characteristics of riluzole after SCI

The pharmacokinetic profile of riluzole was examined using HPLC (Fig. 8A). Riluzole rapidly penetrated into the spinal cords of both injured and uninjured animals. The concentration of riluzole in the uninjured spinal cord was $7.74 \pm 1.46 \mu\text{g/g}$ at 15 min and $10.42 \pm 1.91 \mu\text{g/g}$ at 30 min after a single administration of riluzole at 8 mg/kg. The injured rats had $2.92 \pm 0.53 \mu\text{g/g}$ and $8.31 \pm 0.96 \mu\text{g/g}$ of riluzole in the spinal cord at 15 min and 30 min after injection.

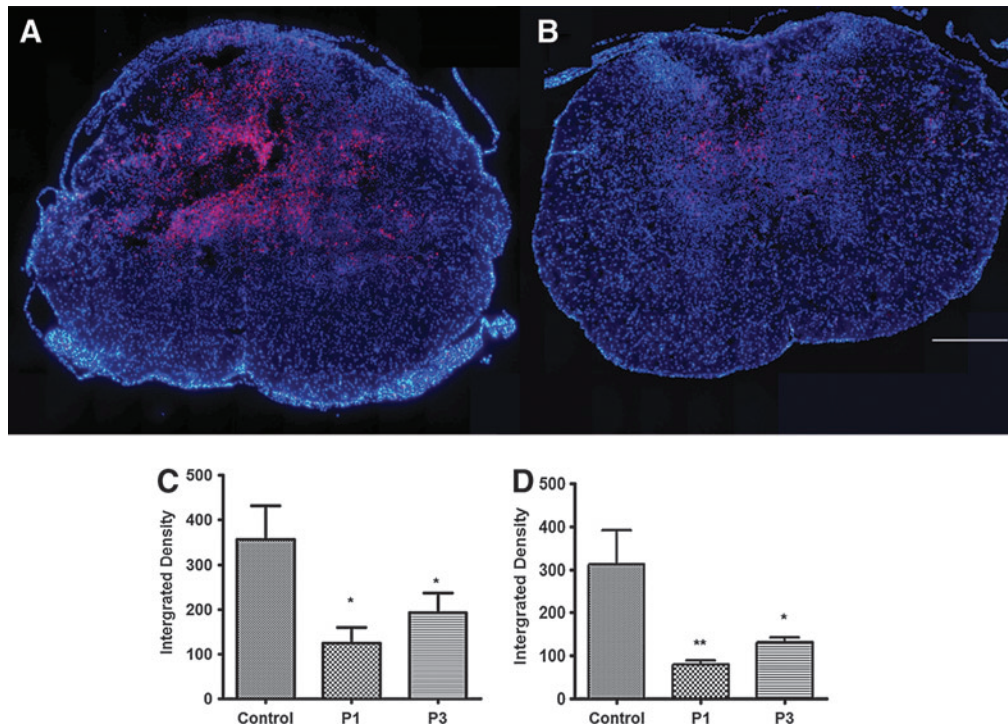


FIG. 6. Immunofluorescence staining of perilesional macrophage/microglia. Diffuse infiltration of Iba1-positive cells was observed at 600 μm caudal to the injury epicenter. A significant decrease was found in Iba1-positive macrophages and microglia at 1 week after SCI in rats that received riluzole 1 h post-SCI (A) compared to control (B). Bar graph illustrating quantitative analysis of the integrated density of Iba1-positive cells in the spinal cord at 1 week (C) and 6 weeks (D) after SCI. There was a significant decrease in Iba1 density in P1 ($p=0.033$) and P3 ($p=0.05$) animals compared to controls at 6 weeks post-SCI. At 1 week post-SCI, the decrease in Iba1 density was significant in P1 rats ($p=0.008$) and P3 ($p=0.041$). Bar = 500 μm .

The concentration of riluzole remained at a high level ($> 10 \mu\text{g/g}$) in the spinal cords for at least 9 h after injection. The pharmacokinetic profile of riluzole in the injured and uninjured spinal cords reached substantially higher levels than those in plasma, with a concentration ratio of 6:1 (Fig. 8B). The pharmacokinetics of riluzole was altered after SCI, with injured rats having a slower elimination compared to the uninjured ones. Riluzole was eliminated from the injured spinal cords with half-lives of 25.1–31.6 h, whereas it was eliminated from the uninjured rats with half-lives of 9.2–10.3 h (Fig. 8C and D).

Repeated administration of riluzole also resulted in a significantly different pharmacokinetic profile in the injured and uninjured rats. Following injury, repeated administration of riluzole resulted in 5.83 $\mu\text{g/mL}$ in plasma and 34.2–38.8 $\mu\text{g/g}$ in the spinal cord. Following the repeated administration protocol in the uninjured control rats, there were 3.21 $\mu\text{g/mL}$ and 16.6–16.7 $\mu\text{g/g}$ riluzole in the plasma and spinal tissue, respectively (Fig. 8E and F). The extent of accumulation from multiple doses was doubled in injured rats, resulting from the prolonged half-life in these animals. This is important as it indicates potentially different pharmacokinetics for this drug in injured patients compared to healthy patients.

Discussion

In this study, we confirm and expand earlier findings that riluzole has significant neuroprotective effects and leads to significant neurobehavioral improvements after cervical SCI. For the first time, using a preclinical animal model, this article demonstrates the effective dose of riluzole that may be administered repeatedly

following cervical SCI without adverse effects on cardiovascular and respiratory functions. After cervical SCI, rats were able to tolerate a repeated administration of 6 mg/kg of riluzole. Also, this study clearly demonstrates the therapeutic time window within which riluzole must be administered after SCI. Initiation of riluzole treatment at 1 and 3 hour post-injury leads to improved locomotor and sensory-motor function, improved axonal conduction, tissue sparing, preserved structural integrity, and transportation in axons, as well as reduced inflammation and apoptosis without increased neuropathic pain. This study also demonstrates that the pharmacokinetic profile of riluzole in injured animals was significantly different from that in their healthy counterparts. Riluzole had a prolonged half-life and delayed elimination in the injured rats compared to the uninjured group of rats. This report provides critical information for the translation of riluzole for the treatment of SCI. In particular, the pharmacokinetic data will be vital for the translation of this drug.

Riluzole is an FDA-approved drug for the treatment of ALS.⁶ It is a benzothiazole anticonvulsant and a non-inactivating voltage-dependent sodium channel inhibitor. Na^+ influx through voltage-gated Na^+ channels is a critical step in the axon injury cascade that follows SCI. Na^+ accumulation leads to Ca^{2+} accumulation via reversal of the $\text{Na}^+-\text{Ca}^{2+}$ exchanger.²⁶ Glutamate can be released by the reverse operation of Na^+ dependent transporters, in turn activating a variety of other receptors, further exacerbating the overload of cellular Ca^{2+} . This Ca^{2+} overload stimulates a variety of Ca^{2+} -dependent enzyme systems (e.g., calpains, phospholipases), leading to structural and functional injury.²⁷ The neuroprotective effects of riluzole appear to result from a blockade of

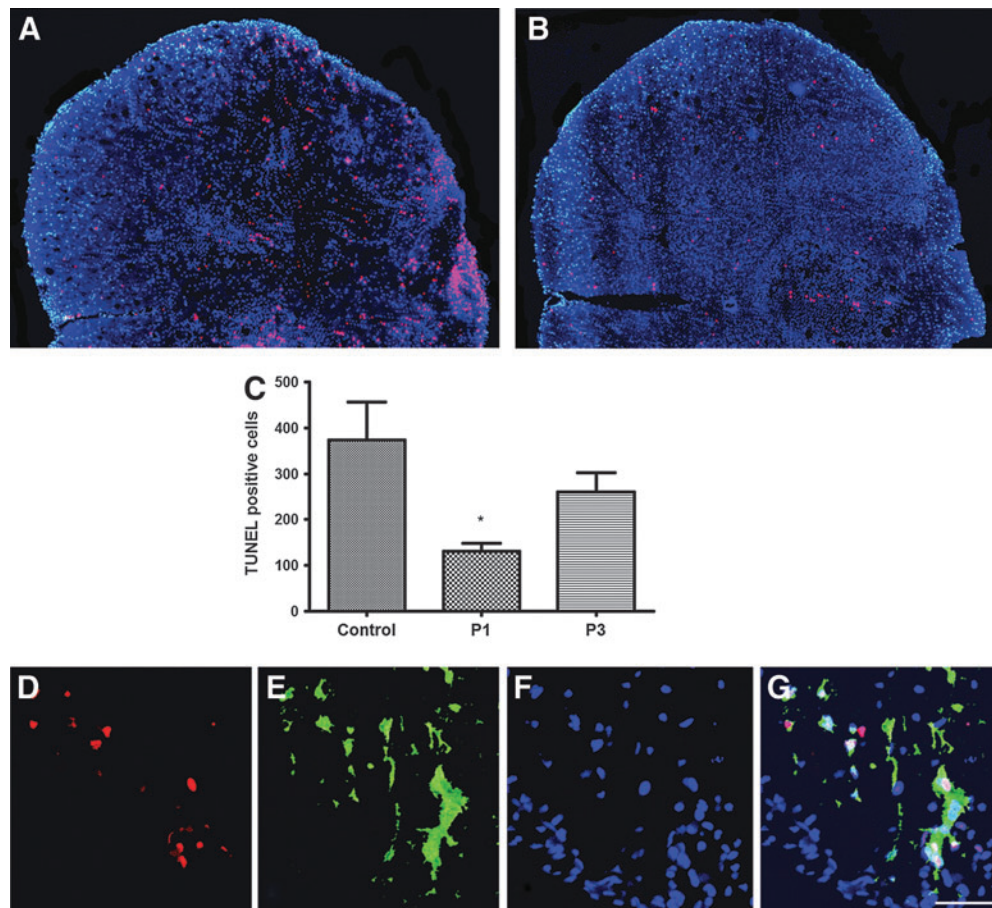


FIG. 7. Riluzole administration reduced apoptosis following SCI. Panels (A) and (B) are representative sections taken 700 μm caudal to the epicenter from a riluzole treated (P1) and control animal, respectively. Sections were immunostained with TUNEL (red) and counterstained at 7 days after SCI. Quantitative analysis revealed a significant decrease in TUNEL-positive cells in the riluzole treatment group (P1) versus control group ($p=0.024$) as shown in bar graph (C). Riluzole treatment at 3 h post-injury (P3) did not show significant reduction in apoptosis ($p=0.492$). A portion of apoptotic cells in the white matter was co-localized with CC1 labeled oligodendrocytes (D–G).

sodium channels whose persistent activation following injury has been associated with degeneration of neural tissue, and by preventing of reversal of Na^+ /calcium (Ca^{2+}) exchanger. In addition, riluzole is anti-glutamatergic via the inhibition of glutamate release, modulation of glutamate receptors (NMDA and AMPA), and the increase of glutamate uptake.^{28,29} The stimulation of neurotrophic factor expression by riluzole may also contribute to the neuroprotective effects.^{30,31} The multifaceted effects of riluzole on excitotoxicity and neuromodulation make it a promising neuroprotective treatment option after SCI. These mechanisms are supported by the behavioral, neurophysiological, and histopathological data showing the greatest extent of improvement when riluzole is administered at 1 hour post-injury when injury-induced ionic imbalance is the greatest. In this article, we also report significant improvements when riluzole is administered at 3 hours post-injury.

An initial dose of 8 mg/kg was used in this study to maximize the neuroprotective effect since the first dose is considered the most important for electrolyte balance and reducing glutamate levels. Others have also reported that riluzole at the above dose reduces the extent of cellular damage and neurobehavioral deficits following trauma in rodents.³² As the repeated injection of 8 mg/kg was shown to be toxic in our initial findings, the subsequent doses were reduced to 6 mg/kg. The reduced dose of 6 mg/kg resulted in sig-

nificantly fewer side effects and less toxicity. Furthermore, the above protocol was sufficient to provide neuroprotection following moderate injury of the rodent cervical spinal cord. Hence, this study has revealed 6 mg/kg as an effective dose of riluzole that is also safe. The tolerability of 50 mg to 200 mg of riluzole has been tested in healthy human subjects. However, the dose-dependent effect of this drug is still unknown in a population of spinal cord-injured patients with varying degree of respiratory compromise. As such, this study highlights a need for careful monitoring of the patients' ventilation and respiratory health during riluzole treatment.

One of the key challenges of neuroprotective treatments following traumatic SCI relates to the acute time course of glutamate release and excitotoxicity.³³ Electrolytic imbalance and glutamate toxicity are early events,³⁴ and extracellular glutamate rises to a toxic level within 15 min following SCI.³⁵ Therefore, delayed treatment with riluzole post-SCI will likely result in poor neuroprotection. In this moderate cervical SCI model, a time window of at least 1 h was sufficient for neuroprotection, and 3 h for improved neurobehavioral outcomes post-injury. Riluzole treatment at both 1 and 3 h post-injury lead to significant improvements in locomotor ability. Optimal functional recovery was seen when riluzole treatment was initiated 1 hour following SCI. There is no direct equation to translate the time window from rodents to human. However,

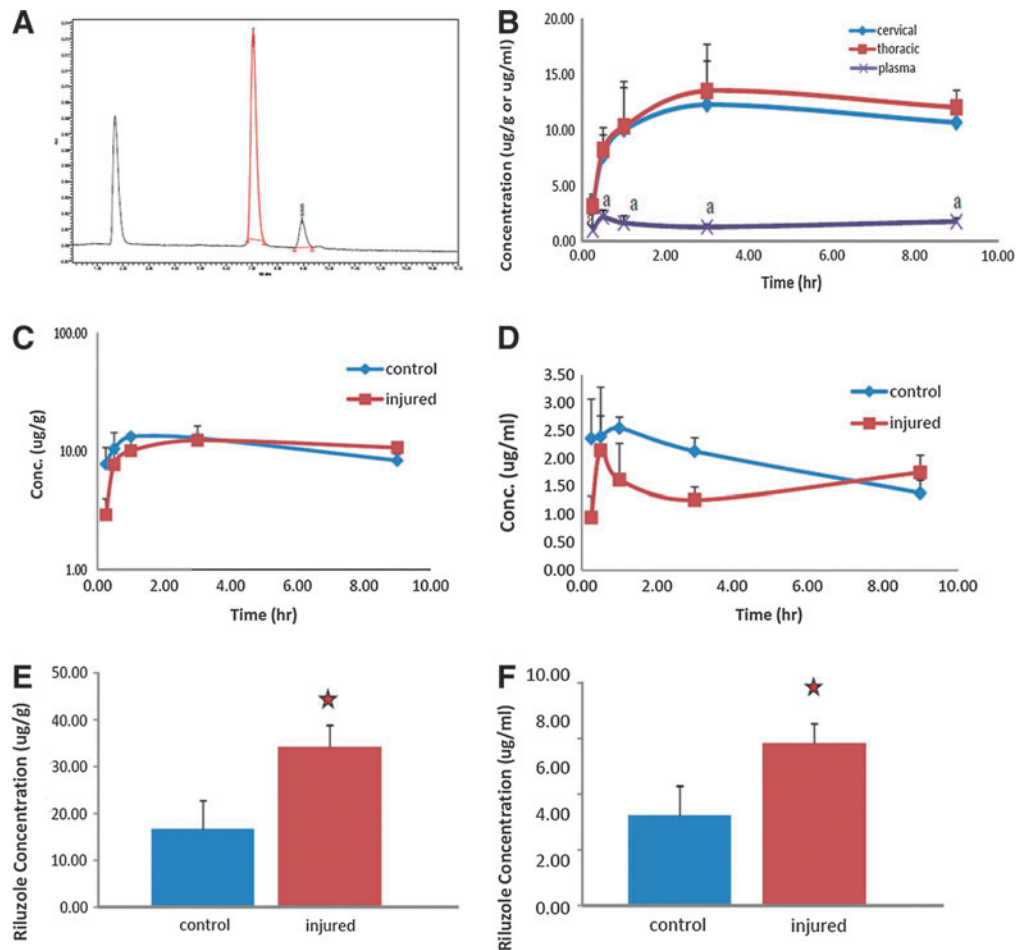


FIG. 8. Pharmacokinetic profile of riluzole. Representative chromatogram of riluzole (A). Pharmacokinetic profile of riluzole in the plasma and in the cervical and thoracic spinal cord segments after SCI (B). Riluzole in spinal cords reached substantially higher levels than that in plasma with a concentration ratio of 6:1. Riluzole penetrated the spinal cord tissue rapidly and reached concentrations of $8.31 \pm 0.96 \mu\text{g/g}$ at 30 min after injection. The pharmacokinetic characteristics of riluzole were altered by the SCI status (C and D). Estimated half-life increased from 9.2–10.3 h in uninjured controls to 25.1–31.6 h in SCI rats. The impact of SCI was further confirmed with the spinal cord and plasma samples from the multiple-dosing regimen (E and F). Concentration of riluzole in the spinal cord tissue of control and injured rats after a 3 day treatment protocol (E). Plasma concentration of riluzole was also significantly higher in the injured rats compared to uninjured controls (F).

indirect information based on metabolic rate differences suggests that the pathological changes 1 h after injury in rats are approximately equal to 4 h post-injury in human. Given that this study also detected improvements when riluzole treatment was initiated 3 h post-injury provides even a wider time point for the initiation of riluzole treatment in patients. Studies examining inflammatory biomarkers after SCI in rodents and human patients suggest many crucial biomarkers are altered earlier in rodents compared to humans.^{36,37} For example, the inflammatory cytokine, IL-6, is increased at 4 h post-SCI in rodents, while this cytokine only peaks at 24–32 h in human subjects. This suggests a difference of 4–6 hours between rodent and human SCI pathology. This 1–3 h time window for riluzole further increases the clinical relevance since a large proportion of existing neuroprotective compounds have no reported post-injury time window. This report expands on our earlier findings, and for the first time describes the time-dependent effects of riluzole following cervical SCI.

Riluzole treatment 1 h after injury resulted in improvement of BBB scores from 10.25 ± 0.41 to 11.42 ± 0.15 , a modest enhancement. The BBB scale system is not linear and the scale

within the 8–14 range is not very sensitive.^{38,39} Furthermore, the BBB assessment scale was initially designed with the thoracic injury model of SCI. Since one of the key objectives of this study was to determine the effect of riluzole in a more clinically relevant cervical model of SCI in rats, we employed the BBB subscore and gridwalk tests. The latter two assessments are more sensitive and clearly demonstrated riluzole's ability to improve neurobehavioral outcome following cervical SCI at both time points. It was noted that a higher proportion of the rats in the P1 group were able to achieve a BBB score of 12, indicating the ability of the animals to attain occasional forelimb–hindlimb coordination. This may be explained by the greater preservation of the vestibulospinal and reticulospinal tracts in the treated animals as revealed by the retrograde labeling experiment. The increased number of preserved spinal tracts in the treatment groups is also consistent with the higher amount of NF200 in the P1 group compared to controls. These observations suggest that the structural integrity of the spinal cord really is protected by riluzole. It is believed that less than 10% of the original axonal population is necessary for functional recovery after SCI;¹⁶ hence, even a small increase in

the number of surviving axons may lead to significant improvements in functional outcomes.

Prior to this study, very little was known about the pharmacokinetics of riluzole in rats. As such, this study provides vital information for the preclinical investigation of this drug for various models of trauma to the central nervous system. The pharmacokinetic profile of riluzole is different in injured and control animals. The elimination of riluzole was delayed in the injured rats, resulting in doubling the half-life of riluzole in these rats compared to healthy controls. The concentrations of riluzole in the plasma and central nervous system were also much higher in the injured rats. This may help to explain the toxic effects of repeated administration of riluzole at 8 mg/kg. In contrast, 8 mg/kg of riluzole was tolerated well without significant adverse effects in the uninjured rats. Edema, electrolyte disturbances, derangements of energy metabolism, biochemical changes, altered blood flow, and changes in microvascular permeability are all parts of the secondary injury cascade that follows the initial trauma to the spinal cord.³⁸ The pharmacokinetic changes seen in these animals may have been due to the compromised circulation system and metabolic status of SCI animals. This finding reinforces the importance of close monitoring of pharmacokinetics in SCI patients during clinical trials and the necessary adjustment of the riluzole administration accordingly. Special care should be taken when monitoring cervical spinal cord injured patients enrolled in clinical trials. Overall, the findings here will be of use to inform clinicians and researchers as riluzole is brought closer to being licensed for treatment of SCI.

Author Disclosure Statement

No competing financial interests exist.

References

- Sekhon LH, and Fehlings MG. (2001). Epidemiology, demographics, and pathophysiology of acute spinal cord injury. *Spine* 26, S2–12.
- Tator CH, and Fehlings MG. (1991). Review of the secondary injury theory of acute spinal cord trauma with emphasis on vascular mechanisms. *J Neurosurg* 75, 15–26.
- Park E, Velumina AA, and Fehlings MG. (2004). The role of excitotoxicity in secondary mechanisms of spinal cord injury: A review with an emphasis on the implications for white matter degeneration. *J Neurotrauma* 21, 754–774.
- Tator CH, Hashimoto R, Raich A, Norvell D, Fehlings MG, Harrop JS, Guest J, Aarabi B, and Grossman RG. (2012). Translational potential of preclinical trials of neuroprotection through pharmacotherapy for spinal cord injury. *J Neurosurg Spine* 17, 157–229.
- Schwartz G, and Fehlings MG. (2002). Secondary injury mechanisms of spinal cord trauma: A novel therapeutic approach for the management of secondary pathophysiology with the sodium channel blocker riluzole. In: *Progress in Brain Research*. L. McKerracher, G. Doucet, S. Rossignol (eds), Elsevier Science B.V., pps. 177–190.
- Miller RG, Mitchell JD, Lyon M, and Moore DH. (2003). Riluzole for amyotrophic lateral sclerosis (ALS)/motor neuron disease (MND). *Amyotroph Lateral Scler Other Motor Neuron Disord* 4, 191–206.
- Azbill RD, Mu X, and Springer JE. (2000). Riluzole increases high-affinity glutamate uptake in rat spinal cord synaptosomes. *Brain Res* 871, 175–180.
- Doble A. (1996). The pharmacology and mechanism of action of riluzole. *Neurology* 47, S233–241.
- Coderre TJ, Kumar N, Lefebvre CD, and Yu JS. (2007). A comparison of the glutamate release inhibition and anti-allodynic effects of gabapentin, lamotrigine, and riluzole in a model of neuropathic pain. *J Neurochem* 100, 1289–1299.
- Springer JE, Azbill RD, Kennedy Se, George J, and Geddes JW. (1997). Rapid calpain I activation and cytoskeletal protein degradation following traumatic spinal cord injury: Attenuation with riluzole pretreatment. *J Neurochem* 69, 1592–1600.
- Stutzman JM, Pratt J, Boraud T, and Gross C. (1996). The effect of riluzole on post-traumatic spinal cord injury in the rat. *Neuroreport* 7, 387–392.
- Schwartz G, and Fehlings MG. (2001). Evaluation of the neuroprotective effects of sodium channel blockers after spinal cord injury: Improved behavioral and neuroanatomical recovery with riluzole. *J Neurosurg* 94, 245–256.
- Mu X, Azbill Rd, and Springer JE. (2000). Riluzole improves measure of oxidative stress following traumatic spinal cord injury. *Brain Res* 870, 66–72.
- Ho Ch, Wuermser LA, Priebe MM, Chiodo AE, Sclenza WM, and Kirshblum SC. (2007). Spinal cord injury medicine. 1. Epidemiology and classification. *Arch Phys Med Rehabil* 88, S49–54.
- Krassioukov A. (2009). Autonomic function following cervical spinal cord injury. *Respir Physiol Neurobiol* 169, 157–164.
- Fehlings MG, and Tator CH. (1995). The relationships among the severity of spinal cord injury, residual neurological function, axon counts, and counts of retrogradely labeled neurons after experimental spinal cord injury. *Exp Neurol* 132, 220–228.
- Basso DM, Beattie MS, and Bresnahan JC. (1995). A sensitive and reliable locomotor rating scale for open field testing in rats. *J Neurotrauma* 12, 1–21.
- Karimi-Abdolrezaee S, Eftekharpour E, Wang J, Morshead CM, and Fehlings MG. (2006). Delayed transplantation of adult neural precursor cells promotes remyelination and functional neurological recovery after spinal cord injury. *J Neurosci* 26, 3377–3389.
- Karimi-Abdolrezaee S, Eftekharpour E, Wang J, Schut D, and Fehlings MG. (2010). Synergistic effects of transplanted adult neural stem-progenitor cells, chondroitinase, and growth factors promote functional repair and plasticity of the chronically injured spinal cord. *J Neurosci* 30, 1657–1676.
- Bruce JC, Oatway MA, and Weaver LC. (2002). Chronic pain after clip-compression injury of the rat spinal cord. *Exp Neurol* 178, 33–48.
- Oatway MA, Chen Y, Bruce JC, Dekaban GA, and Weaver LC. (2005). Anti-CD11d integrin antibody treatment restores normal serotonergic projections to the dorsal, intermediate, and ventral horns of the injured spinal cord. *J Neurosci* 25, 637–647.
- Matsumoto H, Kumon Y, Watanabe H, Ohnishi T, Shudou M, Ii C, Takahashi H, Imai Y, and Tanaka J. (2007). Antibodies to CD11b, CD68, and lectin label neutrophils rather than microglia in traumatic and ischemic brain lesions. *J Neurosci Res* 85, 994–1009.
- Baptiste DC, Austin JW, Zhao W, Nahirny A, Sugita S, and Fehlings MG. (2009). Systemic polyethylene glycol promotes neurological recovery and tissue sparing in rats after cervical spinal cord injury. *J Neuropathol Exp Neurol* 68, 661–667.
- Millane A, Tortolano L, Fernandez C, Bensimon G, Meininger V, and Farinotti R. (2009). Brain and plasma riluzole pharmacokinetics: effect of minocycline combination. *J Pharm Pharm Sci* 209–217.
- Schumacher PA, Eubanks JH, and Fehlings MG. (1999). Increased calpain I-mediated proteolysis, and preferential loss of dephosphorylated NF200, following traumatic spinal cord injury. *Neuroscience* 91, 733–744.
- Agrawal SK, and Fehlings MG. (1996). Mechanisms of secondary injury to spinal cord axons in vitro: role of Na⁺, Na⁽⁺⁾-K⁽⁺⁾-AT-Pase, the Na⁽⁺⁾-H⁺ exchanger, and the Na⁽⁺⁾-Ca²⁺ exchanger. *J Neurosci* 16, 545–552.
- Stys PK. (2005). General mechanisms of axonal damage and its prevention. *J Neurol Sci* 233, 3–13.
- Kretschmer BD, Kratzer U, and Schmidt WJ. (1998). Riluzole, a glutamate release inhibitor, and motor behavior. *Naunyn Schmiedeberg Arch Pharmacol* 358, 181–190.
- Farber NB, Jiang XP, Heinkel C, and Nemmers B. (2002). Anti-epileptic drugs and agents that inhibit voltage-gated sodium channels prevent NMDA antagonist neurotoxicity. *Mol Psychiatry* 7, 726–733.
- Palace J. (2008). Neuroprotection and repair. *J Neurol Sci* 265, 21–25.
- Zarate CA, and Manji HK. (2008). Riluzole in psychiatry: A systematic review of the literature. *Expert Opin Drug Metab Toxicol* 4, 1223–1234.
- McIntosh TK, Smith DH, Voddli M, Perri BR, and Stutzmann JM. (1996). Riluzole, a novel neuroprotective agent, attenuates both neurologic motor and cognitive dysfunction following experimental brain injury in the rat. *J Neurotrauma* 13, 767–780.

33. Agrawal SK, Theriault E, and Fehlings MG. (1998). Role of group I metabotropic glutamate receptors in traumatic spinal cord white matter injury. *J Neurotrauma* 15, 929–941.
34. Liu D, Thangnipon W, and McAdoo DJ. (1991). Excitatory amino acids rise to toxic levels upon impact injury to the rat spinal cord. *Brain Res* 547, 344–348.
35. Kwon BK, Stammers AM, Belanger LM, Bernardo A, Chan D, Bishop CM, Slobogean GP, Zhang H, Umedaly H, Giffin M, Street J, Boyd MC, Paquette SJ, Fisher CG, and Dvorak MF. (2010). Cerebrospinal fluid inflammatory cytokines and biomarkers of injury severity in acute human spinal cord injury. *J Neurotrauma* 27, 669–682.
36. Stammers AT, Liu J, and Kwon BK. (2012). Expression of inflammatory cytokines following acute spinal cord injury in a rodent model. *J Neurosci Res* 90, 782–790.
37. Metz GA, Merkler D, Dietz V, Schwab ME, and Fouad K. (2000). Efficient testing of motor function in spinal cord injured rats. *Brain Res* 883, 165–177.
38. Basso DM. (2004). Behavioral testing after spinal cord injury: Congruities, complexities, and controversies. *J Neurotrauma* 21, 395–404.
39. Rowland JW, Hawryluk GW, Kwon B, and Fehlings MG. (2008). Current status of acute spinal cord injury pathophysiology and emerging therapies: Promise on the horizon. *Neurosurg Focus* 25, E2.

Address correspondence to:
Michael G. Fehlings, MD, PhD, FRCSC
University of Toronto
Toronto Western Hospital
4th Floor West Wing Room 449
399 Bathurst Street
Toronto M5T 2S8
Ontario
Canada

E-mail: Michael.Fehlings@uhn.on.ca